PHYSICAL REVIEW B VOLUME 60, NUMBER 8 15 AUGUST 1999-II

Observation of guided longitudinal acoustic modes in hard supported layers

M. Chirita, R. Sooryakumar, and Hua Xia*
Department of Physics, The Ohio State University, Columbus, Ohio 43210

O. R. Monteiro and I. G. Brown
Lawrence Berkeley National Laboratory, University of California, Berkeley, California 94720

(Received 3 February 1999)

We report experimental as well as theoretical evidence for the occurrence of a high-frequency acoustic excitation, identified as a longitudinal guided mode, in elastically hard films supported on a soft substrate. While existence criteria related to the transverse and longitudinal sound velocities in the film and substrate argue for strong decay channels into the substrate, the excitation is evident as a clear peak in the Brillouin light scattering spectra. A Green's function formalism accounts for the existence of this excitation and provides insight into its properties as illustrated for diamond-like-carbon layers deposited on silicon.
[S0163-1829(99)50832-1]

The properties of acoustic excitations in supported thin films display characteristically different behaviors that depend on the relative magnitudes of the transverse and longitudinal sound velocities in the film and substrate.[1,2] In the range bounded by the transverse sound velocities of the film (V_F^T) and substrate (V_S^T), the surface Rayleigh and guided Sezawa waves are the primary excitations when $V_F^T < V_S^T$.[3,4] At a higher velocity range between the longitudinal sound velocities of the film (V_F^L) and substrate (V_S^L), the longitudinal guided mode (LGM) exists when $V_F^L < V_S^L$, and is characterized by mode displacements primarily along the film plane and a phase velocity close to V_F^L.[5] Excitations lying within these two distinct transverse or longitudinal velocity bands provide for a complete description of acoustic waves in a soft film on a hard material (i.e., $V_F^T < V_S^T$), and have been extensively studied.[6–10] In the opposite limit, i.e., for hard films deposited on soft substrates ($V_S^T < V_F^T$), only one surface acoustic wave (SAW), identified as the Rayleigh wave, exists in a narrow velocity range limited by V_S^T, provided the film thickness (h) is below a critical value.[1] Beyond V_S^T this mode transforms into an evanescent pseudosurface acoustic wave (pSAW), and eventually approaches the Rayleigh velocity of the film for large h.[1,11] Although additional higher order modes with strong decaying character and phase velocities larger than V_F^T are also predicted,[12] few reports of their detection are available.[11] Thus, in contrast to the rich excitation spectrum offered in soft supported films, the presence of only one localized excitation below V_S^T and the weak cross section associated with higher order modes have attracted few investigations probing the acoustic properties of hard films deposited on soft materials.

In this paper we address the high velocity range in the vicinity of V_F^L and report on a successful observation of the longitudinal guided mode (LGM) in hard films, the counterpart of the LGM found in low-speed films. This finding is intriguing, since in this case, the mode velocity V_{LGM} is greater than both V_S^T and V_S^L, and thus *all* partial waves of this mode can propagate into the substrate. The polarization and phase velocity of the observed LGM in the present Brillouin light scattering study are confirmed by calculating, within a Green's function formalism, the local density of states associated with the long wavelength phonons in thermal equilibrium and their variations with film thickness. This description allows for the dispersion of the high-frequency LGM as well as that of the SAW and pSAW excitations to be evaluated.

Since the predominant contribution to the total displacement field consists of propagating in-plane polarized partial waves, the elasto-optic (EO) mechanism becomes the primary coupling mechanism of the LGM to photons.[5,13] Hence, we selected diamond-like-carbon (DLC) layers deposited on silicon for our light scattering investigation. Moreover, as the ripple mediated scattering from surface excitations is also significant in high-speed DLC, this system is particularly attractive for generally investigating high-frequency acoustics in hard layers. As illustrated below, the findings of this study now make it feasible to quantitatively evaluate the independent elastic constants of a hard supported film by light scattering and hence should also be amenable to other dynamic techniques. Unlike for soft films where Brillouin scattering techniques have had tremendous success,[6–8] such determinations of the elastic properties of hard coatings have, hitherto, been severely restricted due to the limited dispersion of true Rayleigh waves and the general lack of evidence for higher order acoustic excitations.

The diamond-like-carbon (DLC) films used in this investigation were produced by a filtered cathodic vacuum arc as described elsewhere.[14] The voltage selected for the substrate bias was -100 V leading to dense, high sp^3 content and hard DLC films. The thickness of each film was measured to an accuracy of 10 nm by variable wavelength photoreflectivity. The sample thickness were 110, 160, 190, and 320 nm. Transmission electron microscopy of the DLC films showed no evidence of damage at the DLC/Si interface. The Brillouin light scattering (BLS) measurements were performed in a back scattering geometry at room temperature with a tandem Fabry-Perot interferometer operated in a sequential six-pass configuration.[15] Approximately 100 mW of p-polarized $\lambda = 514.5$-nm laser radiation was used to record

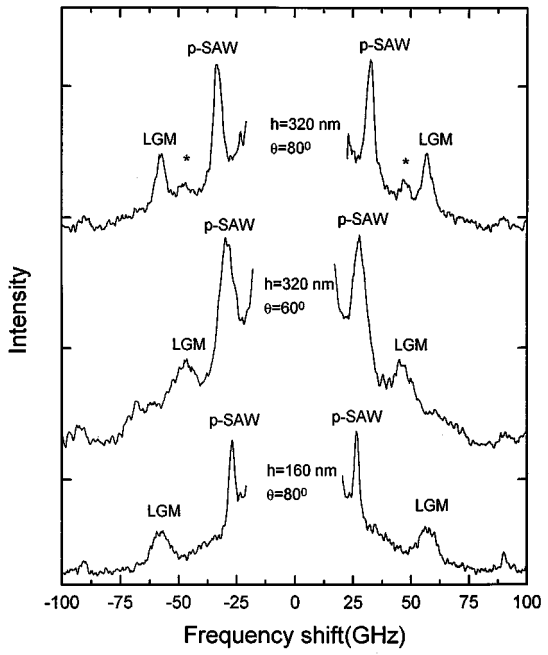

FIG. 1. Brillouin spectra recorded in backscattering from DLC films on Si. The angle of incidence θ and film thicknesses h are as indicated. The modes labeled pSAW, LGM are the pseudosurface and longitudinal guided modes, while $*$ identifies a higher order mode.

the spectra at a typical recording time of 20 min for each spectrum. The dispersion of the phonon velocities was measured by varying the magnitude of $\mathbf{q}h$, the product between the in-plane wave vector $\mathbf{q}$ and film thickness h, through tuning the angles of incidence θ between 40° and 80° as well as studying films of different thicknesses.

Figure 1 shows three typical spectra recorded from two DLC films of thickness $h=320$ nm and $h=160$ nm at $\theta=60°$ and 80°. The strong, lowest frequency (ν_R), peak in each spectrum lying between 26 and 30 GHz is identified as scattering from the pseudosurface wave (pSAW). Consistent with an increasing frequency ν_R with θ, the phase velocity $[V=\nu_R\lambda/(2\sin\theta)]$ of the surface mode increases with qh as illustrated in Fig. 2. It is noted that while the pSAW mode velocity stabilizes at a value lower than the Rayleigh velocity of the film (V_F^R), starting at $qh\sim3$ another wave with velocity V_F^R and whose mode density increases with qh is predicted. The latter excitation and its coupling to pSAW will be discussed elsewhere.[16] The second prominent feature in the data is the mode labeled LGM. It is observed from all films at different angles of incidence θ; the corresponding phase velocities are, within experimental error, independent of qh over the regime probed. In addition, there are weaker peaks, identified by the symbol $*$ in Fig. 1 that are in fact dispersive. The experimental findings are summarized in Fig. 2.

In order to gain insight into the origin, and to evaluate the properties, of these high-frequency excitations, the local phonon mode density $n_i(\omega^2,q,z)$, as well as its value averaged over the film thickness, was evaluated within a Green's function formalism. Here i (1–3) refers to mode polarizations where $i=1,2$ are, respectively, the shear horizontal and sagittally polarized transverse modes, and $i=3$ the longitudi-

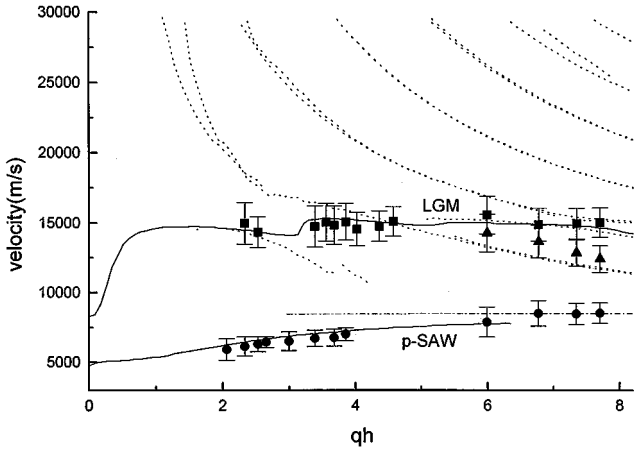

FIG. 2. Calculated dispersion curves for the pSAW and LGM mode are shown as full lines. The dotted lines represent the calculated higher order mode dispersion while the dashed-dotted line corresponds to a mode at the film Rayleigh velocity. Note that beyond $qh\sim6.2$ the latter mode has a significantly larger density of states than that of pSAW. The experimental data are also shown where the circles, squares, and triangles correspond, respectively, to pSAW, LGM, and higher order modes.

nally polarized excitation, ω the mode frequency, and z the distance from the film surface where the mode density is evaluated. In this description n_i is given by the corresponding elastodynamic Green's tensor $G_{ii}(\omega^2,q;z,z')$ via the relation.[17]

$$n_i(\omega^2,q,z)=-(\pi)^{-1}\,\mathrm{Im}\,G_{ii}(\omega^2,q;z,z')|_{z=z'}$$

In evaluating $G_{ii}(\omega+i0,q)$ we follow the method of Every and co-workers[18] where the response of the medium at point z subject to the presence of a fictitious driving δ force $\mathbf{F}$ at point z' is calculated. The displacement field $\mathbf{u}_j(\mathbf{r},t)$, that satisfies the equations of motion in each medium, is written as a linear superposition of partial plane waves. According to linear response theory the wave amplitudes are proportional to the applied force. In the film all six partial waves are considered while in the substrate only the three outgoing waves are retained. The weighting factors corresponding to each partial wave are determined from the boundary conditions satisfied by the σ_{i1} components of the stress tensor at the free surface, interface and at point z', as well as from the continuity of the displacement $\mathbf{u}_j(\mathbf{r},t)$ at the interface and at z'. Expressing the stress tensor components and the force F in terms of their Fourier components with respect to the in-plane position vector $\mathbf{r}_\parallel$ and time t, the boundary condition equations simplify to a system of linear equations that allows for a straightforward determination of the weighting factors. It follows that the displacement field can then be expressed directly in terms of the applied force providing for the elastodynamic Green's tensor through the relation $u_j(\mathbf{r}_\parallel,z,t)=G_{ij}(\mathbf{r}_\parallel,z,t)\;F_j$ leading to the Fourier transform $G_{ii}(\omega+i0,q)$.

The advantages of such an analysis are several. First, the local and integrated density of states for each polarization component can be analyzed for a given frequency, allowing the relative contribution as well as the spatial distribution of each polarization component to be evaluated. Second, peaks

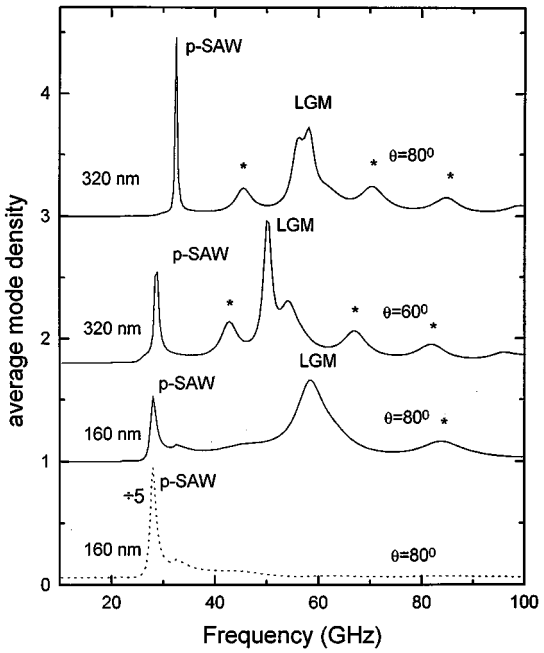

FIG. 3. Calculated density of phonon states in DLC films averaged over the film thickness h, for $h=160$ and 320 nm and angles of incidence $\theta=60°$ and 80°. The full lines are the longitudinal components, the dotted line (scaled down by a factor of 5) the density associated with the transverse componet. The weak peaks (*) are higher order dispersive excitations that correspond to the dotted lines in Fig. 2. Note the mixed character of the pSAW mode and the absence of transverse contributions to the LGM.

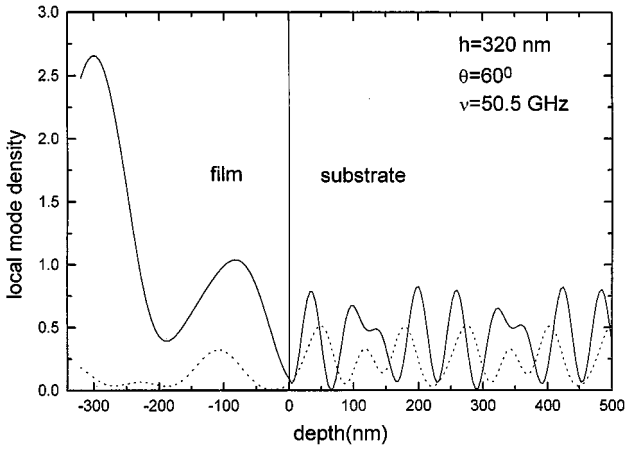

FIG. 4. Spatial distribution of the local density of states for the LGM supported in a DLC film of thickness 320 nm and angle of incidence of 60°. Full line represents the longitudinal component while the transverse component is given by the dotted line. The film substrate interface is located at the origin of the x axis.

in the integrated density of states for different film thicknesses provide for the variation of the phase velocities with qh, thus enabling a direct correlation to the experimental data as illustrated in Fig. 2. This step, hence, overcomes the need for prior knowledge of the EO coefficients to determine mode frequencies via the scattered light intensity. The two independent elastic constants ($C_{11}=614$ GPa; $C_{44}=244$ GPa) of the isotropic DLC layer used in these calculations were obtained from the data as follows: C_{11} is directly deduced from the phase velocity of LGM which is an accurate measure of the longitudinal sound velocity in the film, and the known density of the DLC layer ($\rho_{\mathrm{DLC}}=2.8\,\mathrm{g/cm^3}$). The remaining parameter C_{44} is then deduced from a least-squares fit to the experimental dispersion curve of the pSAW mode utilizing the well-known C_{ij}'s and density of the subtrate Si.

The results of our calculations for the average longitudinal density of states determined by evaluating $G_{33}(\omega,q)$ over the DLC layer thickness are shown as a function of frequency in Fig. 3, where θ and h correspond to those values shown in Fig. 1. Two main features are evident. The peak labeled pSAW with a frequency of ~30 GHz relates to the pseudosurface wave where, for these film thicknesses, at least one of the associated partial waves has an oscillatory component in the substrate. Consistent with the mixed character of the low-frequency pseudosurface excitation, the transverse density of states evaluated through $G_{11}(\omega,q)$ reveals a peak at the same frequency (compare the lowest two curves in Fig. 3, for example) and confirm that the phase velocity (V_{pSAW}) increases with qh as shown by the good fit to data in Fig. 2. The other prominent feature (LGM) in Fig. 3 relates to the longitudinal guided mode which, in agreement with experiment, shows practically no thickness dependence of its velocity for a given θ. Being principally a longitudinally polarized excitation, no significant transverse density of states was found at the frequency ν_{LGM} of the guided mode. This is further borne out in Fig. 4, illustrating the spatial distribution of the local density of states for both polarizations at 50.5 GHz, the calculated (Fig. 3) frequency of ν_{LGM} for a DLC film with $h=320$ nm at $\theta=60°$. The longitudinal mode density at this frequency is found to be largest near the film surface to a depth of ~120 nm. It is this feature that directly contributes to the observation of the LGM in the DLC layers by light scattering. The oscillatory behavior of both longitudinal and transverse components in the substrate is also evident and consistent with two propagating component partial waves.

Guided longitudinal acoustic waves with velocities above V_S^T that propagate in the vicinity of longitudinal acoustic (LA) wave velocity, V_F^L, of the film have been previously reported for single and bilayers when $V_F^T<V_S^T$, i.e., for soft films on hard substrates.[5,13] These low-speed films in which the LGM have been observed share the common characteristic that the phase velocity V_{LGM} is smaller than V_S^L, the LA wave velocity of the substrate. Thus, unlike the DLC/Si system utilized in this study, the substrate LA mode is not a viable decay channel in the low-speed films and the lifetime of the LGM is largely determined by coupling to the shear modes of the subtrate. Since the LGM has only a small shear component, conversion to substrate transverse modes is weak, and thus the longitudinal guided mode remains, not surprisingly, mainly confined to the supported soft layer.

In addition to the prominent peaks, weaker features (identified as *'s) in the longitudinal mode density are also evident in Fig. 3. These modes have comparable transverse components, and correspond to the highly dispersive modes shown as dotted lines in Fig. 2. Although their mode density is in general small, their presence in the DLC layers is evident in the light scattering spectra as indicated by the sym-

bols in Fig. 1, with their dispersive character being sensitive to the sound velocities of the supported films.

In summary, we have presented evidence for the existence of the high-frequency longitudinal guided mode in a supported hard film. Despite being characterized by evanescent partial waves in the substrate, the LGM is clearly evident as a peak in the BLS spectra. The properties of the excitation have been investigated by calculating the associated elastodynamic Green's tensor that allows for the local density of states as well as the mode dispersion to be determined. The findings reported here thus provide a major step in classifying long wave acoustic surface and film excitations in supported films that now exhibit equivalence with respect to high-frequency acoustics in both hard and soft layers. The observation of the LGM in high-speed films allows for a direct means to investigate the longitudinal sound velocity and therefore to determine the C_{11} elastic constant. Thus, the LGM together with pSAW's that are evident in light scattering experiments now open opportunities in the study of high-frequency acoustics as well as the elastic properties of laminar structures and coatings, which place no limitations on the relative magnitudes of the film/ substrate acoustic velocities.

We thank Professor A. Every for providing details of the computer code needed for calculating the Green's function. This work was supported by the U.S. Army Research Office under Grant No. DAAG 55-97-1-0260 and the NSF under Grant No. DMR 97-01685.

*On leave from National Laboratory of Solid State Microstructures, Nanjing University, Nanjing 210093, China.

[1] G. W. Farnell and E. L. Adler, in *Physical Acoustics*, edited by W. P. Mason and R. N. Thurston (Academic Press, New York, 1972), Vol. 9, p. 35.

[2] B. A. Auld, *Acoustic Fields & Waves in Solids* (Wiley, New York, 1973), Vol. 2.

[3] Lord Rayleigh, Proc. London Math. Soc. **17**, 4 (1887).

[4] K. Sezawa and K. Kanai, Bull. Earth. Res. Inst. Tokyo Imperial Univ. **13**, 237 (1935).

[5] B. Hillebrands, S. Lee, G. I. Stegeman, H. Cheng, J. E. Potts, and F. Nizzoli, Phys. Rev. Lett. **60**, 832 (1988).

[6] R. Sandercock, in *Light Scattering in Solids III*, edited by M. Cardona and G. Guntherodt (Springer-Verlag, Berlin, 1982), p. 173.

[7] F. Nizzoli and J. R. Sandercock, in *Dynamical Properties of Solids*, edited by G. K. Horton and A. A. Maradudin (Elsevier, Amsterdam, 1990), Vol. 6, p. 281.

[8] M. Grimsditch, in *Light Scattering in Solids V*, edited by M. Cardona and M. Gunterodt (Springer-Verlag, Berlin, 1989). p. 284.

[9] J. Kushibiki and N. Chibachi, IEEE Trans. Sonics Ultrason. **32**, 189 (1985).

[10] A. Briggs, *Acoustic Microscopy* (Clarendon Press, Oxford, 1992).

[11] A. G. Every, W. Pang, J. D. Comins, and P. R. Stoddart, Ultrasonics **36**, 223 (1998).

[12] A. Akjouj, E. H. Boudouti, B. Djafari-Rouhani, and L. Dobrzynski, J. Phys.: Condens. Matter **6**, 1089 (1994).

[13] F. Nizzoli, C. Byloos, L. Giovannini, C. E. Bottani, G. Ghislotti, and P. Mutti, Phys. Rev. B **50**, 2027 (1994).

[14] S. Anders, A. Anders, I. G. Brown, B. Wei, K. Komvopoulos, J. W. Ager, and K. M. Yu, Surf. Coat. Technol. **68**, 388 (1994).

[15] S. M. Lindsay, M. W. Anderson, and J. R. Sandercock, Rev. Sci. Instrum. **52**, 1478 (1981).

[16] M. Chirita, H. Xia, R. Sooryakumar, O. Monteiro, and I. Brown (unpublished).

[17] E. H. Boudouti, B. Djafari-Rouhani, and A. Akjouj, Phys. Rev. B **55**, 4442 (1997).

[18] A. G. Every, K. Y. Kim, and A. A. Maznev, J. Acoust. Soc. Am. **102**, 1346 (1997); Z. Zhang, J. D. Comins, A. G. Every, P. R. Stoddart, W. Pang, and T. E. Derry, Phys. Rev. B **58**, 13 677 (1998); A. G. Every (private communication)